Translation and Rotation of Penetrants in Ultrapermeable Nanocomposite Membrane of Poly(2,2-bis(trifluoromethyl)-4,5-difluoro-1,3-dioxole-*co*-tetrafluoroethylene) and Fumed Silica

Junyan Zhong, Guoxing Lin, Wen-Yang Wen, and Alan A. Jones*

Carlson School of Chemistry and Biochemistry, Clark University, Worcester, Massachusetts 01610

Scott Kelman and Benny D. Freeman

Department of Chemical Engineering, Center for Energy and Environmental Resources, University of Texas at Austin, 10100 Burnet Road, Austin, Texas 78758

Received October 13, 2004; Revised Manuscript Received February 10, 2005

ABSTRACT: Diffusion of pentane, cyclohexane, and toluene in nanocomposite films of fumed silica and poly(2,2-bis(trifluoromethyl)-4,5-difluoro-1,3-dioxole-*co*-tetrafluoroethylene) is observed by pulse field gradient NMR. The apparent diffusion constant determined in this experiment depends on the time over which the diffusion measurement is made. The pure copolymer and the nanocomposites based on it are inhomogeneous materials phenomenologically similar to a porous system with the fast diffusion domains having an apparent pore size in the micron size range. In this regard the diffusion can be considered to be anomalous with slopes as low as 0.6 in plots of the logarithm of mean-square displacement vs the logarithm of time at short observation times and at lower silica content. The slower diffusing toluene and cyclohexane are influenced to a greater extent by the inhomogeneous structure when motion is considered over the same time. The addition of nanoparticles increases the diffusion constants of the penetrants substantially, and the diffusion constants from NMR are consistent with diffusion constants determined from desorption experiments. At high nanoparticle concentration, the apparent pore size increases and diffusion becomes closer to Fickian. Rotational motion of cylcohexane is characterized by deuterium spin−lattice relaxation time measurements made as a function of temperature on deuterated cyclohexane in the copolymer/nanoparticle composite. Two minima are present in the spin−lattice relaxation data, indicating the presence of two distinct rotational processes. The two processes are interpreted in terms of the presence of two domains just as in the interpretation of the diffusion data. While an increase in nanoparticle concentration increases the apparent diffusion constants at long times, it does not change rotational motion. The increase in translational mobility is attributed to improved connections between the domains.

Introduction

Superglassy polymers such as poly(1-trimethylsilyl-1-propyne) (PTMSP) and poly(4-methyl-2-pentyne) (PMP) have high glass transition temperatures and unexpectedly high gas permeabilities.[1] The high permeability of this type of polymer has attracted considerable interest in the area of membrane separation applications. These polymers have high fractional free volumes and large free volume elements that act as sorption sites. The bulky repeat units of superglassy polymers lead to poorly packed glasses. The presence of large free volume sorption elements, 0.5−0.6 nm, has been detected by positron annihilation lifetime spectroscopy[2] (PALS) and by xenon-129 NMR.[3] These are about twice the size of free volume elements in conventional glassy polymers. Besides the substituted polyacetylenes, a quite different fluoropolymer poly(2,2-bis(trifluoromethyl)-4,5-difluoro-1,3-dioxole-*co*-tetrafluoroethylene) also displays high permeability along with some of the other properties characteristic of a superglass.[4,5]

Recently, the addition of nonporous inorganic nanoparticles to these superglassy polymers has led to increased permeability contrary to simple expectations.[6−9] Fumed silica nanoparticles modify chain packing leading to increased diffusion of penetrants. The modification of the packing is a surface effect with smaller nanoparticles causing more disruption of packing, leading to faster diffusion.[10] PALS indicates a subtle increase in the size of individual large free volume elements[9] that may account for the increase in permeability. Solubility does not change greatly upon addition of the fumed silica nanoparticles in PTMSP and PMP, and so the increase in permeability is largely ascribed to an increase in the diffusion constant[9] in these systems. This latter point has been confirmed by a direct measurement of the self-diffusion constant of pentane in poly(2,2-bis(trifluoromethyl)-4,5-difluoro-1,3-dioxole-*co*-tetrafluoroethylene) with 65% dioxole units (AF1600 DuPont trademark) by pulse field gradient (PFG) NMR.[11] In this case an increase of an order of magnitude in the diffusion constant was observed, which is both striking and promising in terms of potential applications as a separation membrane. Solubility of larger penetrants is modestly increased in AF1600 in contrast to PTMSP and PMP.

While the rapid diffusion in superglassy polymers is significantly enhanced by the addition of the nanoparticles, the diffusion behavior itself is complex. Both pure AF1600[12−14] and AF1600/nanoparticle composites[11] display apparently tortuous penetrant diffusion based on PFG NMR measurements of the self-diffusion constant of pentane. This means that the value of the apparent diffusion constants depends on the length of time over which diffusion occurs in the NMR experiment. At short times corresponding to short length scales, diffusion appears to be faster and then decreases as the time over which diffusion occurs increases. This behavior is

10.1021/ma047880c CCC: $30.25
Published on Web 04/05/2005

characteristic of systems that are porous such as limestone where rapid diffusion occurs within pores and is slowed by contact with walls. AF1600 and other high permeability polymers are not simple porous systems since there are no microscopic, unoccupied regions as there are in limestone. Individual free volume elements of 0.5−0.6 nm are about the size of small molecule penetrants and by themselves do not constitute pores. More likely, there are regions or domains of higher free volume composed of a number of the larger free volume elements observed by PALS,[4,5] and it is these domains that appear porous by supporting faster diffusion. They are bounded by other domains that support slower diffusion and likely contain the smaller 0.3 nm free volume elements typical of common glassy polymers. Just as there are no true pores in these polymer systems, the domains impeding diffusion are not impenetrable as are the walls surrounding pores in limestone. Solubility of the penetrant could be reduced and/or diffusion of the penetrant could be slower; and in combination these factors lead to the behavior of such domains as walls or impediments to diffusion. The size of the domains supporting fast diffusion are near 1 μm in AF1600 according to PFG NMR, which explains the appearance of porous behavior in the PFG NMR experiments, although the only true vacancies in the system are the subnanometer sized free volume elements. It should be noted that the diffusion constant observed at long times in the PFG NMR experiment is consistent[15] with diffusion constants extracted from a combination of solubility and permeability data.

Diffusion in another copolymer system based on ethylene oxide and propylene oxide displays comparable properties:[16] tortuous diffusion with micron scale structure influencing the translational motion. Again there are no micron size pores, but there are regions supporting faster diffusion and regions supporting slower diffusion that in combination lead to behavior reminiscent of truly porous systems. Similarly, in a blend of poly(ethylene oxide) and poly(methyl methacrylate) the apparent diffusion constant decreases as a function of the time over which diffusion is observed.[17] In this blend there is up to 12 orders of magnitude difference between the segmental correlation times of the two polymers, indicating significant dynamic heterogeneity.[18] If limestone is the prototypical porous system, then perhaps these polymer systems should be considered as soft porous systems to distinguish their characteristics from the straightforward porous character of limestone. Computer simulations[19] of apparent diffusion constants based on regions of faster diffusion and higher solubility bounded by regions of slower diffusion and lower solubility lead to diffusion constants which depend on observation time and apparently tortuous diffusion behavior.

Since the complex diffusion is unusually fast in superglassy polymers and dramatically enhanced by the addition of nanoparticles, a careful examination of the nature of translational motion in these systems is warranted. The initial diffusion study involved pentane,[11] and the extension to other penetrants will add to the information on this type of composite membrane. The larger molecules, toluene and cyclohexane, were chosen since the slower diffusion of these penetrants will provide information on a shorter length scale. There are several characteristics of diffusion in the presence of structure in an inhomogeneous system that can be extracted from diffusion measurements. Diffusion is considered tortuous if the apparent diffusion constant decreases to a plateau value in a plot of the diffusion constant vs the time over which diffusion is observed. The other simple case is restricted diffusion where the apparent diffusion constant continues to monotonically decrease as a function of observation time. For tortuous diffusion there is a pathway through the obstruction so long-range diffusion occurs while for restricted diffusion the penetrant is trapped and does not diffuse over macroscopic distances. These characteristics of diffusion can be compared with the behavior observed as nanoparticles are added to AF 1600 and as molecules of different size are added.

In cases where the diffusion is impeded by the inhomogeneous structure of the medium supporting diffusion, the dimensionality of the space through which the penetrant moves can be characterized in terms of fractal dimensions. Fractal dimensions are determined from the slopes of plots of the logarithm of the apparent diffusion constant vs the logarithm of the time over which diffusion is observed in the PFG NMR experiment.

From another point of view, diffusion is considered anomalous if the slope of a plot of the logarithm of the mean-square displacement vs the logarithm of time is less than one where the value of one is observed for simple Fickian or normal diffusion. Plots of this type will be constructed for diffusion in pure AF1600 and in AF1600/fumed silica nanocomposites of varying composition. This will allow the evaluation of the effect of the addition of fumed silica on this aspect of the diffusion process. Since three penetrants are to be examined, the effect of the nature of the penetrant can also be considered in relation to the presence of anomalous diffusion. In particular, the larger penetrants provide information on a shorter length scale for the same time frame in the PFG NMR experiment.

The size of the structure influencing diffusion can be estimated from the dependence of the apparent diffusion constant on the time over which diffusion is observed in the PFG NMR experiment. How does the size of the structure change upon the addition of the nanoparticles? Again the behavior among different penetrants can be compared.

Last, the value of the diffusion constant determined from PFG NMR for toluene in AF1600 and in AF1600 nanocomposites with fumed silica will be compared with those determined from sorption/desorption experiments. The NMR experiment observes diffusion on a length scale of hundreds of nanometers to microns while the sorption/desorption experiment observes diffusion on a length scale of tens of microns. Are the results of the two experiments on diffusion in nanocomposites consistent? A good comparison between NMR and the combination of solubility and permeability data was found for propane[15] in pure AF1600. Examination of all of these aspects of the diffusion process will allow insight into the changes produced by the addition of nanoparticles to the polymer.

Is there another way to characterize the contrast in dynamics in this system other than measurements of translational diffusion? To move in this direction, spin−lattice relaxation measurements are reported here to examine rotational motion of the penetrant molecules. In the original lattice simulation developed by Cicerone, Wagner, and Ediger[20] to study diffusion in a heteroge-

neous glass, rotational motion was related to translational motion by a combination of the Stokes−Einstein equation and the Debye−Stokes−Einstein equation yielding

$$D = \frac{2r^2}{9\tau} \quad (1)$$

D is the diffusion constant, r is the radius of the penetrant molecule, and τ is the rotational correlation time. From this point of view, if there is a domain that supports fast diffusion and another domain that supports slow diffusion, then there should be a short correlation time for rotation in the first domain and a longer time for rotation in the second domain. If dynamics in the two domains differ sufficiently, spin−lattice relaxation might assist in substantiating the contrast in dynamics in this type of system. This connection between rotational and translational motion is most easily grasped in the context of the lattice simulation,[19,20] and the simulation model also provides a context for relating the two types of data.

To obtain spin−lattice relaxation data that can be most directly interpreted in terms of rotational motion, a deuterated penetrant molecule is desirable. In that case, the dominant relaxation mechanism will be quadrupolar relaxation, and other relaxation mechanisms can be neglected. Since the line widths are likely to be large for the penetrant in a high glass transition matrix, a molecule with a single type of deuterium is also desirable to avoid the complexity of overlapping resonances. Deuterated cyclohexane meets these requirements and also has a high deuterium content that will produce good signal to noise.

A proton PFG NMR diffusion study of cyclohexane in PDD/TFE nanocomposites is part of this report so translation and rotation can be directly compared. If diffusion is enhanced by the addition of nanoparticles, what will be the impact on rotational motion? Both the diffusion and spin−lattice relaxation measurements will be made as a function of concentration of fumed silica nanoparticles. It has been suggested that the nanoparticles disrupt the packing of the surrounding polymer, increasing permeability.[7−10] Positron annihilation lifetime spectroscopy indicates a small increase in the size of the larger free volume elements. If a larger free volume element contains a single cyclohexane molecule and nanoparticles increase the size of the element, rotation should be faster as fumed silica concentration is added. This prediction can be checked against the results of the spin−lattice relaxation measurements.

With these factors in mind, the combined translational and rotational information on the dynamics of penetrant molecules in high permeability polymer/nanoparticle composites will be combined to provide new insights into this type of system. The distinctions between the regions of contrasting mobility will be clarified.

Experimental Results

PFG measurements were made on a Varian Inova 400 MHz wide bore NMR spectrometer by observing proton signals from the penetrant in an 8 mm direct detection probe with high gradient capability (up to 1000 G/cm) from Doty Scientific. The duration, δ, of the gradient pulse is 1 ms, and the recycle time is 15 s. A three-pulse stimulated echo sequence is used, and the time Δ over which diffusion occurs in this experiment was varied from a few milliseconds to 1 s. At each value of Δ, the apparent diffusion constant is determined from the initial decay of the echo amplitude as a function of the square of the gradient field strength. The gradient strength is chosen to decrease the echo amplitude by between 10 and 20% for the maximum value of the gradient applied in the diffusion experiment.

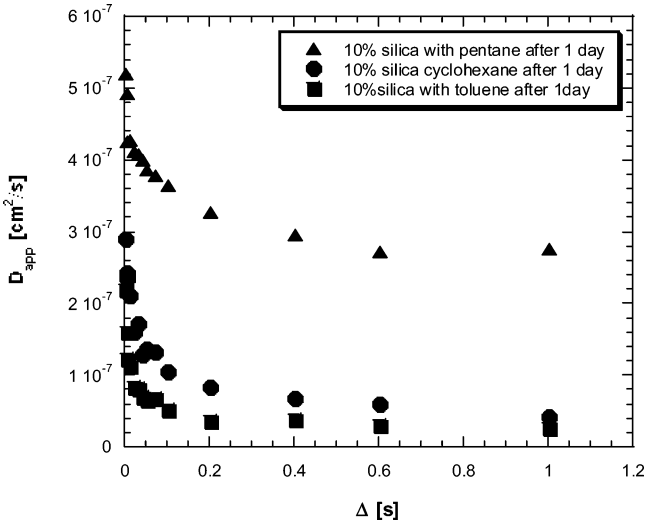

Figure 1. Diffusion constant vs time over which diffusion occurs Δ in the PFG NMR experiment. The triangles are for pentane, circles are for cyclohexane, and squares are for toluene, and all results are for a 10 wt % fumed silica composite film.

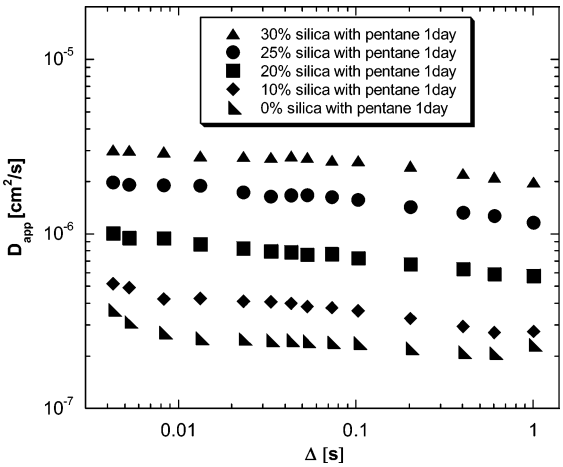

Figure 2. Diffusion constant vs time over which diffusion occurs, Δ, for pentane in fumed silica composite film with a variety of concentrations of silica. The semilogarithmic axes offer a useful perspective on the data with the pentane data changing little at long times especially in the pure polymer.

The nanocomposite is prepared by combining a dilute solution, ~2 wt %, of the copolymer (AF1600 supplied by DuPont) in perfluoroheptane with the fumed silica (CAB-OSIL TS-530 purchased from Cabot) to form a slurry. Rapid stirring is used to disperse the nanoparticles. A film of the slurry is cast and then dried, leading to a clear material. About 8 wt % pentane is added to 0.5 g of film in an 8 mm NMR tube, which is then sealed. For the toluene and cyclohexane samples, 5 wt % is added because the solubility is lower. Also, toluene and cyclohexane diffusion measurements in pure AF1600 could not be made because the solubility is too low.

Figure 1 contains the diffusion constant vs the time over which diffusion occurs, Δ, for toluene, cyclohexane, and pentane in a 10 wt % fumed silica/90 wt % copolymer nanocomposite. The apparent diffusion constants for pentane, toluene, and cyclohexane diffusion are plotted vs Δ in Figures 2, 3, and 4, respectively, at various concentrations of fumed silica in the nanocomposite. Diffusion data are shown for a specific time

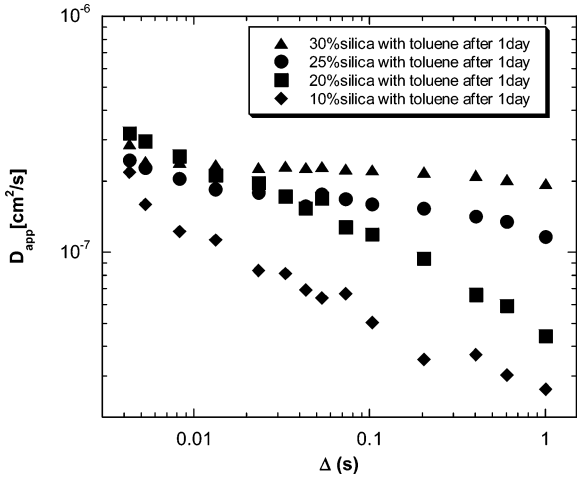

Figure 3. Diffusion constant vs time over which diffusion occurs, Δ, for toluene in fumed silica composite film with a variety of concentrations of silica. The semilogarithmic axes indicate the toluene diffusion constant is still decreasing at long times at low silica concentration.

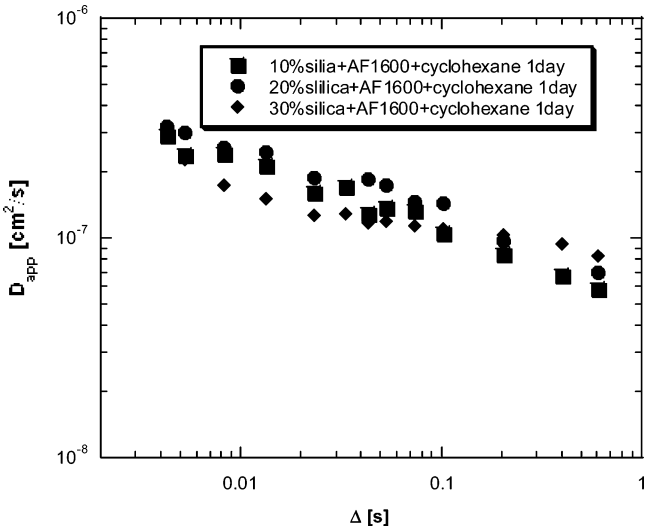

Figure 4. Diffusion constant vs time over which diffusion occurs, Δ, for cyclohexane in fumed silica composite film with a variety of concentrations of silica. The semilogarithmic axes indicate the apparent cyclohexane diffusion constant is decreasing as a function of the time Δ.

of measurement after the addition of penetrant to the film since the films are subject to conditioning and aging effects.[15]

The diffusion constant for cyclohexane in the nanocomposite was also determined from the kinetics of sorption and desorption using a Kahn RG electrobalance in a procedure described elsewhere.[9] The nanocomposite films have a thickness of 25 μm. To compare these data with the results of the PFG NMR experiment, the apparent diffusion constants from the NMR experiment are associated with a length scale given by the equation $\langle r^2\rangle^{1/2} = 6D_{app}\Delta$. The length scale of the sorption/desorption experiment is taken as half the film thickness. The comparison of the NMR data and the desorption data are presented in Figure 5.

Spin−lattice relaxation measurements were performed on two Varian NMR spectrometers. The first is a Varian Inova 400 MHz wide bore spectrometer utilizing a 5 mm static solids broadband solids probe from Chemagnetics. The second is a Varian Mercury 200 MHz narrow bore spectrometer utilizing a 5 mm multinuclear liquids probe. The pulse sequence employed in the spin−lattice relaxation experiments is the traditional inversion−recovery sequence with the recycle time set to 1 s.

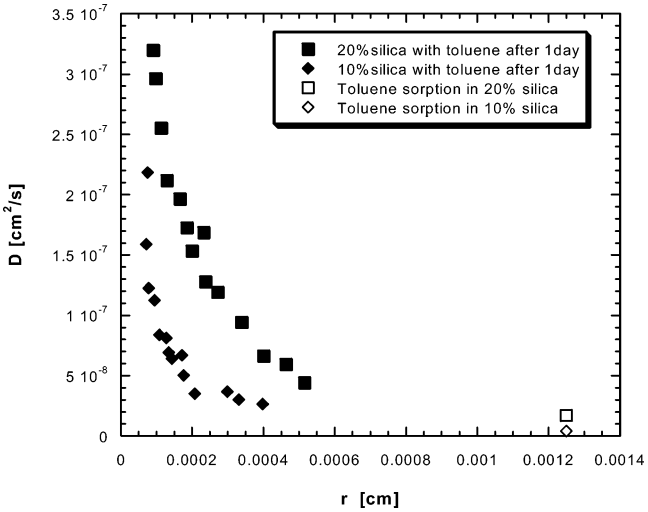

Figure 5. Comparison of NMR and desorption diffusion coefficients as a function of the length scale associated with each of the two experiments. To compare these data with the results of the PFG NMR experiment, the apparent diffusion constants from the NMR experiment are associated with a length scale given by the equation $\langle r^2\rangle^{1/2} = 6D_{app}\Delta$. The length scale of the desorption experiment is taken as one-half the film thickness.

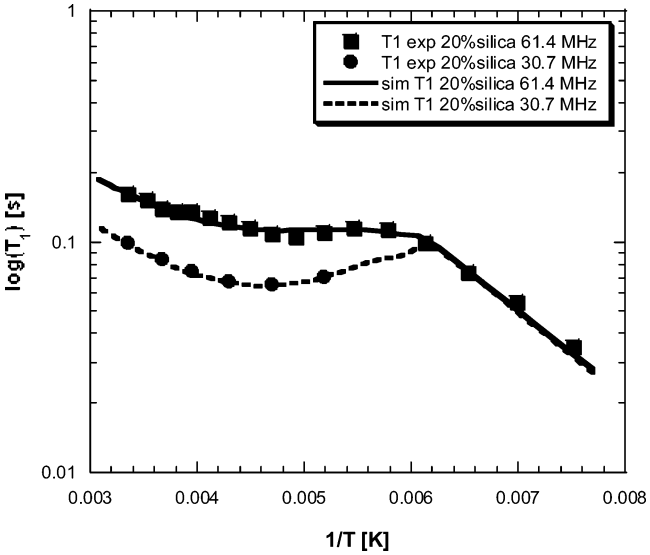

Figure 6. Logarithim of deuterium spin−lattice relaxation times as a function of inverse temperature for deuterated cyclohexane in 20 wt % fumed silica PDD/TFE nanocomposite. The squares are data at 61.4 MHz, and the circles are data at 30.7 MHz. The dashed and solid lines are the interpretations of the data as explained in the text.

The NMR samples for spin−lattice relaxation time measurements were made by adding 5 wt % of deuterated cyclohexane to the nanocomposite film in an NMR tube, and the tube was then sealed. Deuterated cyclohexane was purchased from Aldrich.

Figure 6 shows the plot of the logarithm of deuterium spin−lattice relaxation time, T_1, for cyclohexane in PDD/TFE with 20 wt % fumed silica at deuterium Larmor frequencies of 30.7 and 61.4 MHz as a function of inverse temperature. At the lower Larmor frequency, measurements could not be carried out below −80 °C since the increase in line width of the resonance with decrease in temperature exceeded the sweep width of the spectrometer. At the higher Larmor frequency on the Inova 400 equipped for solids, measurements could be carried out down to −140 °C since wider sweep widths and higher pulse power are available on this spectrometer. Below −140 °C the line shape begins to develop features of the

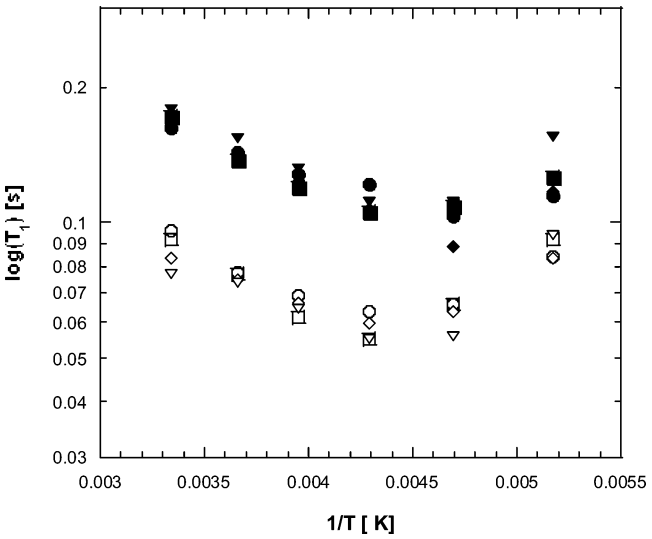

Figure 7. Logarithm of deuterium spin−lattice relaxation times of deuterated cyclohexane as a function of inverse temperature in the vicinity of the higher temperature minimum at various concentrations of fumed silica nanoparticles in the nanocomposite.. Note that the location and depth of the T_1 minimum as a function of temperature is not changing. Filled symbols are data at 61.4 MHz, and open symbols are data at 30.7 MHz. Squares are data for 10 wt % silica; circles, 20 wt %; diamonds, 25 wt %; and triangles, 30 wt %.

quadrupolar line shape where an interpretation based on isotropic rotation is no longer appropriate. Uncertainty in a given determination of T_1 is 10%

Figure 7 shows plots of the logarithm of deuterium spin−lattice relaxation times as a function of inverse temperature at various concentrations of nanoparticles.

Interpretation

In Figure 1, the diffusion data for all three penetrants appear tortuous to the eye in that plateau values are apparently approached, but in Figures 2−4 the logarithmic plots indicate the apparent diffusion constant is still rapidly decreasing for toluene in 10 and 20 wt % silica and cyclohexane at all concentrations of nanoparticles.

The logarithmic displays of the diffusion data as a function of diffusion time in Figures 2−4 allow for a determination of anomalous diffusion behavior. If the diffusion is considered to take place in a fractal space, the fractal dimension of the random walk, d_w, relates the apparent diffusion constant, D_{app}, to Δ, the time over which diffusion occurs according to the equation[16]

$$D_{app} \propto \Delta^{(2/d_w)-1} \quad (2)$$

For normal Fickian diffusion, $2/d_w = 1$, but in the case of anomalous diffusion $2/d_w < 1$. In Figure 2 the logarithm of D_{app} is plotted vs the logarithm of Δ for pentane in PDD/TFE and PDD/TFE nanocomposite with various concentrations of fumed silica. In pure PDD/TFE at small values of Δ, there is a dependence of D_{app} on Δ, but for all the nanocomposites there is only a very weak dependence so that the slopes in these plots are near zero or, equivalently, $2/d_w$ is near one. In Figure 3 similar plots are shown for toluene in the nanocomposites. At the lower concentrations of 10 and 20 wt % fumed silica, there is a significant slope, indicating anomalous diffusion. For toluene in a composite with 20 wt % silica, a value of d_w near three is found. This value of the fractal dimension of the random walk is

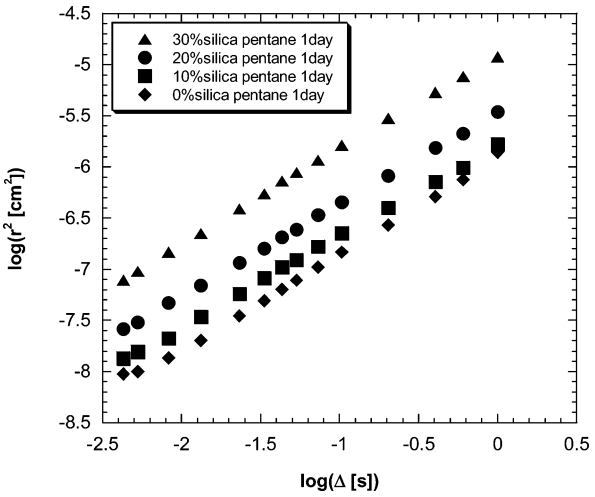

Figure 8. Logarithm of mean-square displacement vs the logarithm of time for pentane in AF1600 and AF1600/fumed silica nanocomposites. Note that the mean-square displacement at a given diffusion time is calculated for the apparent diffusion constant at that time and the time itself.

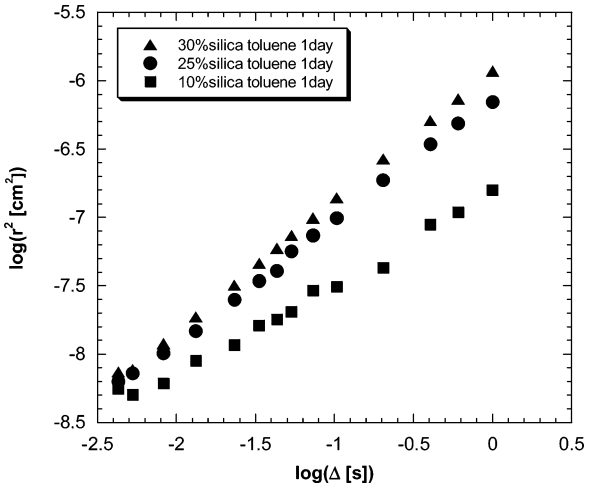

Figure 9. Logarithm of mean-square displacement vs the logarithm of time for toluene in AF1600/fumed silica nanocomposites. Note that the mean-square displacement at a given diffusion time is calculated for the apparent diffusion constant at that time and the time itself.

distinctly different from the value of two for normal diffusion. At higher concentrations of fumed silica, the slope is again reduced, and within experimental error, diffusion approaches normal behavior. In Figure 4 for cylcohexane, there is a significant slope at all concentrations of the silica nanoparticles similar to the slopes observed for toluene in the 20 wt % silica nanocomposite.

Another way to examine the presence of anomalous diffusion is to plot the logarithm of mean-square displacement, $\langle r^2 \rangle = 6D\Delta$, vs the logarithm of the time, Δ. Note that the mean-square displacement at a given diffusion time is calculated for the apparent diffusion constant at that time and the time itself. In this presentation of the data, a slope of one indicates normal or Fickian diffusion while slopes less than one indicate anomalous diffusion. Figure 8 contains plots of this type for pentane while Figure 9 contains plots of this type for toluene. The plots for cyclohexane are similar to the toluene data and are omitted. The behavior for pentane at small Δ for pure PDD/TFE in Figure 8 is different from the behavior at large Δ just as it was in the plot of

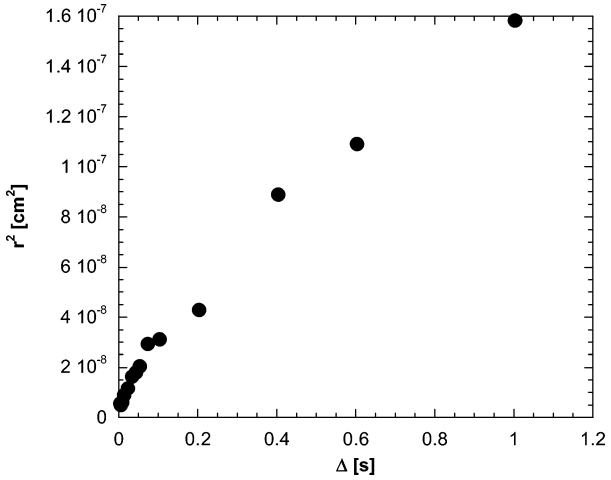

Figure 10. Mean-square displacement vs the time Δ for toluene in a 10 wt % silica nanocomposite. Note that the mean-square displacement at a given diffusion time is calculated for the apparent diffusion constant at that time and the time itself.

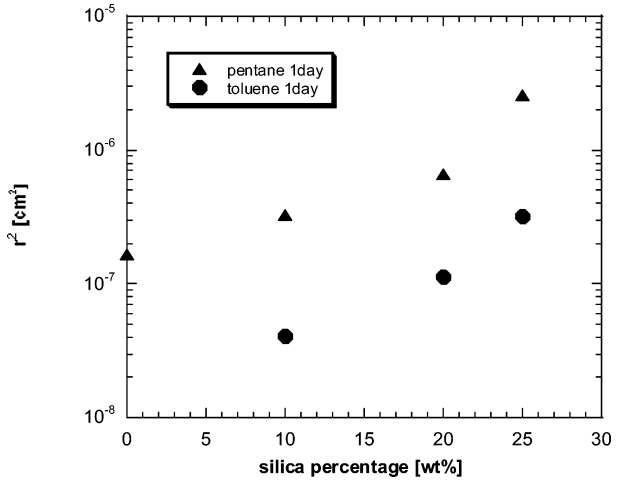

Figure 11. Mean-square size of the domains supporting fast diffusion based on the diffusion pentane and toluene at various loadings of fumed silica. The size is estimated from the point at which the slope changes in plots such as that shown in Figure 10.

Table 1. Initial and Final Slopes from Plots of the Logarithm of Mean-Square Distance vs the Logarithm of Time

	initial slope		final slope	
silica content (wt %)	pentane	toluene	pentane	toluene
0	0.69		0.98	
10	0.81	0.58	0.87	0.78
20	0.89	0.71	0.89	0.51
25	0.96	0.83	0.87	0.87
30	0.93	0.93	0.87	0.92

the logarithm of D_{app} vs the logarithm of Δ in Figure 2. To summarize the changes with the time, Δ, the initial slopes are calculated over the four smallest values of Δ, and final slopes are calculated over the largest five values of Δ. The initial and final slopes of these plots for toluene and pentane are summarized in Table 1. Note that the initial slopes at low concentrations of silica are well below one, especially for toluene, indicative of anomalous diffusion. The initial slopes for cyclohexane are also well below 1, though not included in Table 1. Although there is some scatter, the final slopes are generally higher often approaching 1, indicating that diffusion becomes more Fickian in character as the structure is averaged over at longer times or equivalently longer length scales.

The effect of structure on the diffusion process can be noted in plots of $\langle r^2 \rangle$ vs Δ, such as that shown in Figure 10 for the diffusion of toluene in a film of PDD/TFE with fumed silica. The points rise rapidly at small Δ, and then the rate of increase slows at larger Δ. The point at which the slope changes is associated with a slower increase is a rough measure of the dimensions of the domain associated with fast diffusion. If the first few points are fit to a straight line and the last few points are fit to a straight line, the intersection of the two lines can give an estimate of $\langle r^2 \rangle$ that can be used as a measure of the domain size associated with fast diffusion. In Figure 11, this measure of domain size is plotted as a function of the concentration of fumed silica in the film for both pentane and toluene.

Turning to an interpretation of the spin−lattice relaxation in terms of rotational motion, the relaxation times at 61.4 MHz shown in Figure 6 as a function of inverse temperature indicate the presence of two T_1 minima. There is a broad minimum clearly visible at about 220 K in the data at both field strengths. In addition to the presence of the minimum, there is a large separation between the T_1 values at the two Larmor frequencies at temperatures above the minimum that indicates a broad distribution of correlation times. At temperatures below the minimum, the T_1 values at high and low Larmor frequency become similar. At even lower temperatures, there is a dramatic drop in the values at the higher Larmor frequency, indicating the presence of a lower temperature minimum. Overall, this is unusual relaxation behavior that cannot be described by the typical approach involving a single broad distribution of relaxation times. In view of the evidence for two minima in Figure 6, two dynamic processes with rather different basic time scales will be required for a quantitative interpretation. This apparent bimodal spin−lattice relaxation behavior is qualitatively consistent with the diffusion data. Both can be interpreted in terms of two domains in the nanocomposite with differing translational[19,20] and rotational dynamics with exchange of the penetrant between the domains.

Frequently the Kohlrausch−Williams−Watts (KWW) correlation function is used to analyze relaxation data in polymers. A modified form is used to interpret spin−lattice relaxation data[21,22] in terms of isotropic reorientation and librational motion. This approach has been used to describe reorientation produced by segmental motion in a polymer backbone, but here the reorientation is the result of rotation of the penetrant in the glassy matrix. Cyclohexane can also undergo conformational interchanges in polymer matrices, but the time scale of this motion is too slow to contribute to spin−lattice relaxation.[23−25] The modified KWW function,[21,22] $G(t)$, has the form

$$G(t) = a_{lib} \exp\left[\frac{-t}{\tau_{lib}}\right] + [1 - a_{lib}] \exp\left[-\left(\frac{t}{\tau_{rot}}\right)^{\beta}\right] \quad (3)$$

where a_{lib}'s correspond to amplitudes of librational motion, τ_{lib} is the correlation time for librational motion, τ_{rot} is the correlation time for rotational reorientation, and β determines the distribution of correlation times. The parameter β ranges from 0 to 1, and a smaller value leads to a broader distribution of exponential correlation times.

Table 2. Spin−Lattice Relaxation Interpretational Parameters for Deuterated Cyclohexane in 20 wt % Fumed Silica PDD/TFE Nanocomposite

dynamic mode	P	a_{lib}	β	τ_{inf} (ps)	B	T_0
slow	0.15	0.44	0.185	0.1	460	120
fast	0.85	0.27	0.865	0.1	380	0

When there is a single T_1 minimum for a polymer system, eq 2 is usually adequate to interpret the relaxation data. With the presence of two minima in the data under consideration here, two modified KWW correlation functions can be combined with weighting factors P_1 and P_2:

$$G(t) = P_1G_1 + P_2G_2$$

$$G_i(t) = (a_{lib})_i \exp\left[\frac{-t}{(\tau_{lib})_i}\right] + [1 - (a_{lib})_i] \exp\left[-\left(\frac{t}{(\tau_{rot})_i}\right)^{\beta_i}\right] \quad i = 1, 2 \quad (4)$$

This assumes the penetrant molecules exchanges between the two domains, and this is also assumed in the lattice simulation[19,20] that produces the dependence of the apparent diffusion constant on the time over which diffusion is observed of the type shown in Figure 1.

For numerical purposes, the stretched exponential is expanded into a distribution of exponential correlation times.

$$\exp\left[-\left(\frac{t}{(\tau_{rot})_1}\right)^{\beta_1}\right] = \sum_i \rho_1(\tau_{1i}) \exp\left(-\frac{t}{\tau_{1i}}\right)$$

$$\exp\left[-\left(\frac{t}{(\tau_{rot})_2}\right)^{\beta_2}\right] = \sum_i \rho_2(\tau_{2i}) \exp\left(-\frac{t}{\tau_{2i}}\right) \quad (5)$$

The spectral density is given by

$$J(\omega) = \int_0^\infty G(t) \exp(-i\bar{\omega}t)\, dt \quad (6)$$

The rotational correlation time is given a Vogel−Tamman−Fulcher (VTF) temperature dependence

$$\tau_{rot} = \tau_\infty \times 10^{[B/(T - T_0)]} \quad (7)$$

where τ_∞ is the usual prefactor, the parameter B is related to the activation energy, and T_0 is the Vogel temperature. When $T_0 = 0$, the correlation times revert to a simple Arrhenius temperature dependence.

The average correlation time for rotational dynamics, $\tau_{rot,c}$, is given by

$$\tau_{rot,c} = \frac{\tau_{rot}}{\beta}\Gamma\left(\frac{1}{\beta}\right) \quad (8)$$

T_1 can then be expressed as

$$\frac{1}{T_1} = \frac{3}{10}\pi^2(e^2qQ/h)^2[J(\omega_D) + 4J(2\omega_D)] \quad (9)$$

The quadrupole coupling constant e^2qQ/h is set at 172 kHz for the deuterons on cyclohexane, and the deuterium Larmor frequency is indicated by ω_D.

The fit of the spin−lattice relaxation data at both Larmor frequencies for cyclohexane in the PDD/TFE nanocomposite with 20 wt % silica is shown in Figure 6. The parameters producing the fit are given in Table 2.

Discussion

From a qualitative standpoint, the diffusion of pentane, cyclohexane, and toluene in PDD/TFE and PDD/TFE/ fumed silica nanocomposites is apparently tortuous. However, the apparent diffusion constants for toluene in the 10 and 20 wt % fumed silica nanocomposites and cyclohexane in all concentrations of nanoparticles do not even really approach a plateau, as can be best seen in Figures 2−4. However, if measurements could be made at longer times, a plateau would be expected. Because of the relatively slow toluene diffusion, no average over structure influencing diffusion is reached in the time scale studied. The length scales covered by the diffusion experiment are significantly smaller in the case of toluene because diffusion is slow. In Figure 5, the apparent diffusion constants from NMR are compared with diffusion constants from desorption. For this comparison, a length scale is used for each experiment, and the data appear to be consistent although the desorption data are on a length scale that is 2−3 times larger than the largest length scale in the NMR data. Also, the rapid increase in the apparent size of the structure with increasing nanoparticle content, as seen in Figure 11, requires more time to achieve an average, especially for the slower diffusing toluene.

Toluene might be expected to diffuse at a significantly decreased rate relative to pentane because the diameter of toluene is somewhat greater than the larger of the free volume elements. This places a more severe restriction on the available space in the case of toluene translational dynamics and that leads to the smaller apparent size of the fast diffusing domains for toluene relative to pentane, as seen in Figure 11. Thus, the structure determined in these diffusion experiments is quite dependent on the penetrant molecule in the PFG NMR experiment. In this case, structure depends on dynamics, which is not a conventional situation.

Another way of viewing this is through the apparent tortuosity, which can be measured by the ratio given by the apparent diffusion constant at small values of Δ over the apparent diffusion constant at large values of Δ. For pentane this ratio is around 2, for cyclohexane it is 5 or 6, and for toluene at low silica content it is 10. Thus, over the range of the measurements, toluene motion slows significantly as it finds a pathway through the domain structure. Also as seen in Figure 3, the apparent diffusion constant for toluene at small Δ is about the same at all concentrations of nanoparticles while the case for pentane is quite different in Figure 2. At all values of Δ, the apparent diffusion constants for cyclohexane are quite similar at all concentrations of silica. Thus, at small Δ, toluene is diffusing inside a fast diffusing domain at all concentrations of nanoparticles, but the size of the domain is smaller at low concentrations of fumed silica so the diffusion slows rapidly. Much less slowing occurs at high nanoparticle concentration since the space in which toluene can move rapidly is larger. All the cyclohexane data may be in the fast domain regime, and only at the very largest values of Δ is an average over the structure beginning to be achieved.

The fractal dimension of the random walk of 3 is less than the value of 4 that is observed for curvilinear diffusion such as that seen for the Doi−Edwards reptation model in regime III.[26] In some computer simulations of defects in glasses, stringlike structures of defects were observed.[27] If diffusion occurred along a stringlike

structure that had a random walk character, then one might expect the diffusion of the penetrant to be curvilinear and have a slope of −0.5 or a fractal random walk dimension of 4. The lower fractal dimension of the random walk observed for toluene at lower nanoparticle content indicates a different fractal space but not so different. It is unfortunate that measurements of toluene diffusion in pure PDD/TFE could not be made because the polymer without nanoparticles would be more directly comparable to the computer simulations.[27] Pentane diffusion is too fast so that measurements would have to be made at smaller values of Δ to best observe the structure influencing pentane diffusion in pure PDD/TFE. On the other hand, cyclohexane is too slow to achieve the long-range averaging. Some caution should be used in considering diffusion as occurring in some space because there is no sharp boundary between domains, and there will be a distribution of dynamics in both domains. However, since the penetrant dynamics display features like a porous system with sharp boundaries, it is useful to employ interpretational formalisms developed for the better defined systems.

The slopes of the data plotted in Figures 8 and 9 give an alternative view of the nature of diffusion that is consistent with the characterization of anomalous diffusion using the exponent d_w. In pure PDD/TFE, pentane has a low initial slope and a higher final slope. At small values of Δ, the pentane diffusion has not averaged over the structure and appears anomalous with a slope of 0.69 that rises to a slope of 0.98 at large Δ when the diffusion has become normal after averaging over the structure. For toluene at 10 wt % silica, the initial slope is 0.58 and rises to 0.78. In this case, the toluene does not diffuse far enough to achieve a normal character even at large values of Δ. This is also a case where the fractal dimension is near 3. At higher silica content, the initial slope increases and the fractal dimension drops to near 2. For cyclohexane, the initial slope and the final slope are in the range of 0.6−0.8, indicating the long-range averaging is not achieved. Both views of the diffusion process indicate the addition of nanoparticles makes the diffusion appear closer to normal, which we attribute to a better interconnectedness of the space through which diffusion occurs rapidly. Even without calculations, the eye can see the slope for 10 wt % fumed silica in Figure 9 is lower than for 25 and 30 wt %. Also note in Figure 8 for pentane that the slope in this case of pure PDD/TFE visually appears to increase at larger values of Δ.

In all of this consideration of diffusion in the nanocomposites, one question remains. Why is the structure influencing diffusion so large? The root-mean-square radius is about 0.8 μm for the fast diffusing domain based on toluene in the 10 wt % fumed silica nanocomposite. All estimates of size for the other situations are larger either at higher nanoparticle content or in the case of pentane. As one moves from pure polymer to high nanoparticle content, one may be shifting from structure that reflects the heterogeneous copolymer glass to structure that reflects the impenetrable nanoparticle itself. The nanoparticles used in this study have a diameter of 200−300 nm, but they are fractal particles themselves. The large dimensions seen at high nanoparticle content could well be associated with the nanoparticles. Note in Figure 11 that the size of the mobile domain deduced from toluene diffusion is smaller than it is for pentane diffusion. Thus, the structure inferred from this experiment depends on the probe molecule.

The high permeability polymers are sometimes referred to as nanoporous materials,[1] but the structure of the so-called pores is not clearly defined and in fact the PFG NMR experiment is one of the few approaches available to examine this point. Still, the characterization of the domain structure given here based on dynamics does not lead to a clear picture of the source of the structure influencing the dynamics. Since the permeability is high based on the macroscopic approach of observing the penetrant cross a film, the pore structure must allow for rapid, long-range diffusion if high permeability is to be achieved. In fact, in the AF2400 copolymer with higher (87%) dioxole content, the diffusion is faster than in AF1600. In AF2400, diffusion also appears normal rather than tortuous,[15] most likely because the fast diffusion domains are so well interconnected that structure could only be observed at smaller values of Δ than are accessible in most high gradient NMR spectrometers. It is only in the less porous PDD/TFE that the pore structure can be observed in the PFG NMR experiment. Other factors may contribute to the observation of large pore dimensions. Certainly there is a distribution of sizes since the polymers are amorphous glasses. The nature of the process of averaging over structures of various sizes in the PFG NMR experiment is not established, so possibly it is heavily influenced by the presence of a few larger structures. Since the penetrant can enter the areas acting as walls where slower diffusion occurs, this may serve to slow diffusion more than a wall that is impenetrable and reflects a penetrant. Even within fast diffusing regions there is a distribution of diffusion constants, but the analysis is based on the value of a single effective diffusion constant.

The spin−lattice relaxation data at two different frequencies and as a function of temperature allow for a more detailed interpretation of the distribution of time scales. The presence of two minima associated with two reorientational processes is consistent with the interpretation of translational motion in terms of two regions or domains with distinctly different translational motion. It is only fortuitous that the two time scales of the rotational dynamics are so well separated that two minima are observed in the spin−lattice relaxation experiment. This does allow for a characterization of the distribution of correlation times for each domain. Figure 12 displays the average reorientational correlation time for both modes as a function of temperature. At room temperature, rotational dynamics of the two modes are separated by about 3 orders of magnitude. If the dynamic components were closer in time so that they overlapped, the bimodal aspect could have been more difficult to identify. A plot of the distribution of exponential correlation times vs correlation time for each of the two dynamic modes is presented in Figure 13. This figure shows how much the two distributions differ in character with a narrow fast mode visually dominating the broad slow mode.

The parameters associated with the description of the faster and slower rotational components given in Table 2 are informative. The population, P, associated with the faster domain is larger. This is sensible since the domain containing more large free volume elements would be better able to accommodate the cyclohexane molecule. The distribution of correlation times associ-

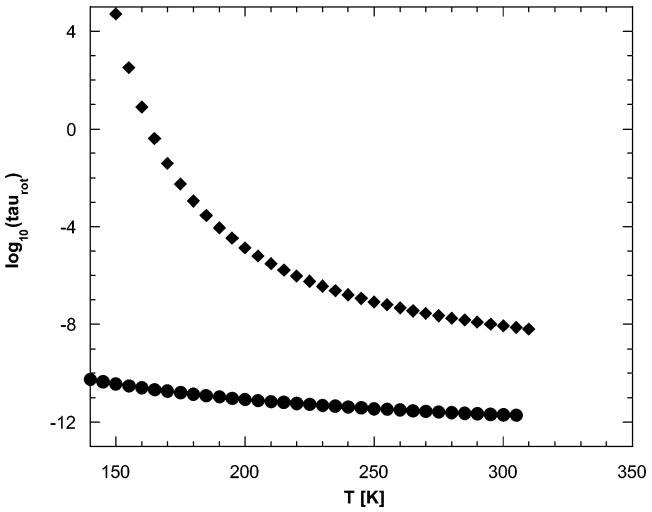

Figure 12. Average rotational correlation time of cyclohexane for each mode as a function of temperature for 20 wt % fumed silica PDD/TFE nanocomposite. The points are not data but the result of the interpretation of the spin−lattice relaxation data.

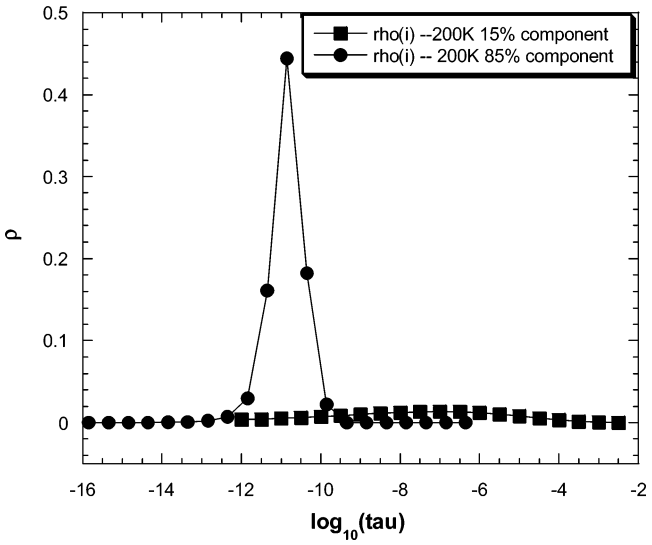

Figure 13. Distribution of correlation times given by ρ_i vs τ_i at 200 K for cyclohexane in 20 wt % fumed silica PDD/TFE nanocomposite. Both the narrow fast mode (filled circles) and the broad slow mode (filled squares) are shown. The points are not data but the result of the interpretation of the spin−lattice relaxation data.

ated with the faster motion is narrow, reflecting less coupling to the polymer matrix. The lack of significant coupling to the matrix also is consistent with an Arrhenius temperature dependence. The slower component has a smaller weighting factor associated with a lower solubility in the domains containing the smaller free volume elements. Lower solubility is consistent with this domain acting as a barrier to diffusion according to the results of the lattice simulation of diffusion in a heterogeneous matrix.[19] Slower translational motion in this domain also contributes to the barrier characteristics,[19] and according to the interpretation, dynamics are 3 orders of magnitude slower in this domain at room temperature. The broad distribution of correlation times in this domain indicates a stronger coupling of the dynamics to the matrix, consistent with smaller free volume elements as is the Vogel−Tamman−Fulcher temperature dependence.

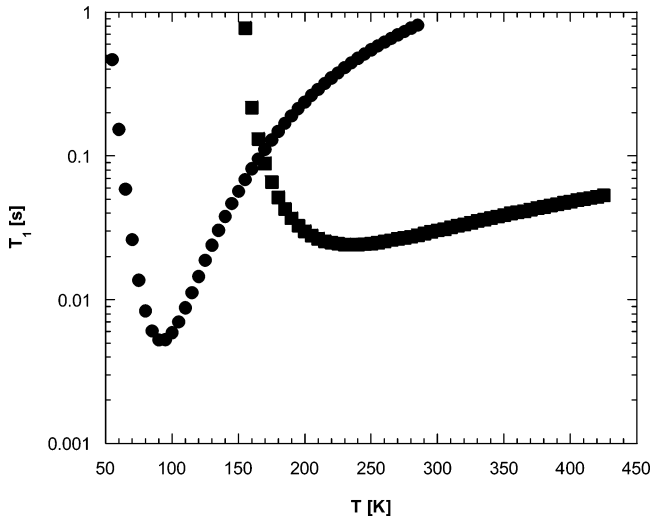

Figure 14. Spin−lattice relaxation times at 61.4 MHz calculated for each of the two modes separately. The points are not data but the result of the interpretation of the spin−lattice relaxation data.

The combination of these two rotational processes leads to the rather unusual dependence of spin−lattice relaxation on temperature seen in Figure 6. At higher temperatures, spin−lattice relaxation has a strong dependence on Larmor frequency, and at lower temperatures the spin−lattice relaxation times become nearly coincident. At higher temperatures, the relaxation is dominated by the slower motions since they are close to the Larmor frequency and are described by a broad distribution. At low temperatures, the faster process becomes close to the Larmor frequency. It is described by a narrow distribution of correlation times so spin−lattice relaxation no longer has a significant dependence on Larmor frequency. Spin−lattice relaxation calculated from each of the two modes separately is shown in Figure 14 to help understand the contributions of the two dynamic components to the observed spin−lattice relaxation. The overall behavior with a significant Larmor frequency dependence at high temperature and little dependence at low temperature can only be produced by a bimodal distribution of correlation times.

The lower temperature minimum is not as well characterized since the data do not traverse the minimum. The line shape begins to take on structure associated with the quadrupolar interaction below about 130 K. A spectrum displaying developing quadrupolar features is shown in Figure 15. At the temperatures of the spin−lattice relaxation measurements, the line shape is Lorentzian in nature with widths less than 10 kHz. At temperatures below 130 K, deuterium solid echo line shape experiments would be a suitable approach to further characterize reorientational dynamics, and this work will be carried out in the future.

It should be pointed out that rapid rotation of the cyclohexane in the polymer/nanoparticle matrix continues well below the freezing point of pure cyclohexane, which is at 279 K. This implies the absence of large clusters of cyclohexane that could organize into a crystal, consistent with the picture of isolated molecules located in individual free volume elements.

In Figure 7, the spin−lattice relaxation times at several concentrations of nanoparticles are presented. There is little change in the relaxation behavior across the temperature range studied. This implies that rota-

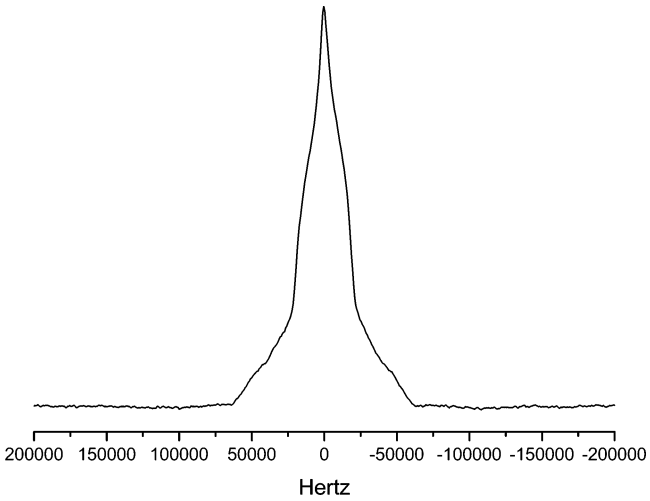

Figure 15. Deuterium line shape at 133 K. The line shape is no longer Lorentzian since features involving the quadrupole coupling are emerging at this temperature.

tional motion is not significantly altered by changing levels of nanoparticles. On the other hand, the data in Figures 2−4 clearly show an increase in translational motion at long times as nanoparticle concentration is raised. For pentane and toluene, the increase in the apparent diffusion with nanoparticle concentration is greaterthan for cyclohexane. However, the apparent diffusion constants in Figure 4 for cyclohexane are still decreasing at the longest times used in the experiments. The change in apparent diffusion constant with nanoparticle concentration could be larger if measurements at longer times were available. Nevertheless, diffusion is increasing as nanoparticle concentration is raised while the rate of rotation is not changing. In view of the relationship between rotation and translation expressed in eq 1, this appears to be contradictory. However, it is diffusion over greater distances at larger times, Δ's, that is increasing in Figure 3. This can be produced by an improvement in the connections between domains supporting facile translation. Within one of these domains, rotation and translation are not significantly changing. This would imply that the size of individual free volume elements is not changing greatly so that rotational motion is not changing either. The increase in translational motion over larger distances is controlled by the morphology of the domain structure rather than the nature of the individual free volume elements.

All rotational and translational motion presented in Figures 1−4 is for a specific time after sample preparation. Translational motion in high permeability polymers and nanocomposites based on these polymers is subject to conditioning and aging.[15] Shortly after pentrants are added to the film, diffusion increases in PFG NMR measurements.[15] This is observed for cyclohexane in the films studied here. However, spin−lattice relaxation times did not change with time after the addition of the penetrant. If rotation is not changing and translation is changing, then it is again the interconnections between domains that are altered by the conditioning induced by the addition of the penetrant and not the size of the individual free volume elements contained in the domains.

A quantitative connection between translation and rotation can be made using eq 1. At 300 K in the 20 wt % silica film, the fast rotational correlation time is 2 ps and the slow rotational is 9 ns. Using eq 1 and a radius of 0.58 nm for cyclohexane,[28] $D_{fast} = 9 \times 10^{-5}$ cm^2 s^{-1} and $D_{slow} = 2 \times 10^{-8}$ cm^2 s^{-1}. The apparent diffusion constant at the longest time measured (1000 ms) is 5×10^{-8}cm^2 s^{-1}, which indicates faster motion. The apparent diffusion constant at long times is an average over the fast and slow domains, so it is reasonable for it to have a higher value. Also, the diffusion constants are still decreasing as shown in Figure 4, so it may still decrease if even longer times could be used in the measurement. At the other extreme, the apparent diffusion constant at the shortest time (4 ms) is 3×10^{-7} cm^2 s^{-1}, which is 2 orders of magnitude smaller than the diffusion constant calculated from the fast rotational correlation time. In fact, the diffusion constant for pure cyclohexane is 1.43×10^{-5} cm^2 s^{-1}, which is a factor of 3 smaller than the value calculated from the fast rotational correlation time. The diffusion constant calculated for the fast region may actually not be a reasonable concept since the fast rotational motion could be occurring in a single large free volume element of about the same dimensions as the cyclohexane molecule and therefore not be associated with a region in which translational motion occurs. If a rotational correlation time is calculated from the diffusion constant of pure cylcohexane using eq 1, a value of 13 ps results. Thus, rotation of cyclohexane in a large free volume element is faster than in pure cyclohexane. This could be possible if the motion is considered to be occurring in a hole with dimensions larger than the molecule.

Values of the librational contribution to both the slow and the fast processes are individually listed in Table 2. However, the librational time constant is 0.1 ps for both so the librational contribution could be merged into a single total value equal to $P_1 a_{lib1} + P_2 a_{lib2}$. The separation of the two librational components is not certain, and so the total librational contribution to spin−lattice relaxation may be the better defined quantity.

Conclusions

Diffusion of pentane and toluene in AF1600 and in nanocomposites based on this copolymer with fumed silica appears to be occurring in a porous material with micron sized pores. There are no true pores of this magnitude in these systems, but the appearance of porous behavior is attributed to the presence of domains that support fast diffusion bounded by domains which support slow diffusion. Toluene and cyclohexane diffusion in AF1600/fumed silica nanocomposites is anomalous and can be viewed as occurring in a fractal space at lower concentrations of nanoparticles. Pentane diffusion in the same nanocomposites displays some of the aspects of anomalous diffusion, but the faster translational motion of pentane allows for an averaging over the inhomogeneous structure of the nanocomposites at longer times. In all cases, the addition of the fumed silica to the polymer substantially increases the apparent diffusion constant and increases the apparent size of the structure influencing diffusion. This system has "soft" or penetrable walls and involves distributions of motional rates, so using the language of true porous systems may be imprecise. Still, much of the dynamic behavior resembles true porous systems, and thus the concepts applied to such systems offer at least a starting point for characterization.

Spin−lattice relaxation times indicate rotational motion of the cyclohexane in the nanocomposites is bimodal

in nature with a separation in time of about 3 decades near room temperature. The two dynamic modes are associated with two domains in the copolymer/nanoparticle composite. This domain structure involving differences in rotational dynamics is consistent with the apparent diffusion constants depending on the time over which diffusion is observed. Increases in nanoparticle concentration lead to more rapid diffusion but do not significantly alter rotational dynamics. The increase in diffusion over longer length scales at longer observation times is the result of improved connections between domains supporting rapid translation. In a similar fashion, conditioning of the nanocomposite after the addition of penetrant increases translational motion but not rotational motion by improving the interconnections between the domains supporting faster transport.

The size of the domains is in the micron range according to the diffusion experiment. This is very large, and there is no conventional characterization of this domain structure. With only the dynamics based characterization of the structure given here, there is still some uncertainty in the underlying identity of the domain structure. Diffusion probes this structure, but the domain size and interconnectivity differ depending on the probe molecule. It is reassuring that the spin−lattice relaxation data indicate bimodal dynamics, providing some confirmation of the interpretation used to interpret the diffusion data. In some sense, the superglassy polymers including AF1600 appear to have a pore structure, as has long been inferred from pemeability,[1] but the underlying nature of the pores or domains supporting fast dynamics still needs further characterization. The rapid diffusion in these systems certainly arises from the presence of the large free volume elements. However, since these are less than a nanometer in size, it is proposed that the domain structure indicated by the NMR experiments is the result of clustering of the large free volume elements to produce the observed micron-sized structure.

Acknowledgment. This research was carried out with the financial support of the National Science Foundation (Grant DMR-0209614).

References and Notes

(1) Nagai, K.; Masuda, T.; Nakagawa, T.; Freeman, B. D.; Pinnau, I. *Prog. Polym. Sci.* **2001**, *26*, 721−798.
(2) Yampolskii, Yu. P.; Shantarovich, V. P. In *Polymer Membranes for Gas and Vapor Separation*; ACS Symposium Series No. 733; Freeman, B. D., Pinnau, I., Eds.; American Chemical Society: Washington, DC, 1999; p 102.
(3) Wang, Y.; Inglefield, P. T.; Jones, A. A. *Polymer* **2002**, *43*, 1867−1872.
(4) Merkel, T. C.; Bondar, V. I.; Nagai, K.; Freeman, B. D.; Yampolskii, V. *Macromolecules* **1999**, *32*, 8427−8440.
(5) Alentiev, A. Y.; Shantarovich, V. P.; Merkel, T. C.; Bondar, V. I.; Freeman, B. D.; Yampolskii, Y. P. *Macromolecules* **2002**, *35*, 9513−9522.
(6) Pinnau, I.; He, Z. Filled Superglassy Membrane. U.S. Patent No. 6,316,684, 2001.
(7) Merkel, T. C.; Freeman, B. D.; Spontak, R. J.; He, Z.; Pinnau, I.; Meakin, P.; Hill, A. J. *Science* **2002**, *296*, 519−522.
(8) Merkel, T. C.; Freeman, B. D.; He, Z.; Pinnau, I.; Meakin, P.; Hill, A. *J. Chem. Mater.* **2003**, *15*, 109−123.
(9) Merkel, T. C.; He, Z.; Pinnau, I.; Freeman, B. D.; Meakin, P.; Hill, A. J. *Macromolecules* **2003**, *36*, 8406−8414.
(10) Andrady, A. L.; Merkel, T. C.; Toy, L. G. *Macromolecules* **2004**, *37*, 4329−4331.
(11) Zhong, J.; Wen, W.-Y.; Jones, A. A. *Macromolecules* **2003**, *36*, 6430−6432.
(12) Meresi, G.; Wang, Y.; Cardoza, J.; Wen, W.-Y.; Jones, A. A.; Inglefield, P. T. *Macromolecules* **2001**, *34*, 1131−1133.
(13) Meresi, G.; Wang, Y.; Cardoza, J.; Wen, W. Y.; Jones, A. A.; Gosselin, J.; Azar, D.; Inglefield, P. T. *Macromolecules* **2001**, *34*, 4852−4856.
(14) Wang, Y.; Meresi, G.; Gosselin, J.; Azar, D.; Wen, W.-Y.; Jones, A. A.; Inglefield, P. T. *Macromolecules* **2001**, *34*, 6680−6683.
(15) Zhang, J.; Klebanov, B.; Inglefield, P. T.; Jones, A. A. *Macromolecules* **2002**, *35*, 7725−7729.
(16) Hayamizu, K.; Akiba, E.; Bando, T.; Aihara, Y.; Price, W. S. *Macromolecules* **2003**, *36*, 2785−2792.
(17) Cao, H.; Lin, G.; Jones, A. A. *J. Polym. Sci., Polym. Phys.* **2004**, *42*, 1053−1067.
(18) Lutz, T. R.; He, Y.; Ediger, M. D.; Cao, H.; Lin, G.; Jones, A. A. *Macromolecules* **2003**, *36*, 1724−1730.
(19) Lin, G.; Zhang, J.; Cao, H.; Jones, A. A. *J. Phys. Chem. B* **2003**, *107*, 6179−6186.
(20) Cicerone, M. T.; Wagner, P. A.; Ediger, M. D. *J. Phys. Chem. B* **1997**, *101*, 8727−8734.
(21) Min, B. C.; Qui, X. H.; Ediger, M. D.; Pitsikalis, M.; Hadjichristidis, N. *Macromolecules* **2001**, *34*, 4466−4475.
(22) Lutz, T. R.; He, Y.; Ediger, M. D.; Cao, H.; Lin, G.; Jones, A. A. *Macromolecules* **2003**, *36*, 1724−1730.
(23) Heiboer, J. Ph.D. Thesis, University of Leyden, 1972.
(24) Laupretre, F.; Virlet, J.; Bayle, J.-P. *Macromolecules* **1985**, *18*, 1846−1850.
(25) Zhao, J.; Jones, A. A.; Inglefield, P. T.; Bendler, J. T. *Polymer* **1998**, *39,* 1339−1344.
(26) Doi, M.; Edwards, S. F. *The Theory of Polymer Dynamics*; Clarendon: Oxford, 1986.
(27) Donati, C.; Douglas, J. F.; Kob, W.; Plimpton, S. J.; Poole, P. H.; Glotzer, S. C. *Phys. Rev. Lett.* **1998**, *80*, 2338−2341.
(28) Magalhaes, F. D.; Laurence, R. L.; Conner, Wm. C. *J. Phys. Chem. B* **1998**, *102*, 2317−2324.
(29) Mitzithras, A.; Cveney, F. M.; Strange, J. H. *J. Mol. Liq.* **1992**, *54*, 273−281.

MA047880C